

# Novel Crystalline Microporous Transition-Metal Phosphites $M_{11}(\text{HPO}_3)_8(\text{OH})_6$ ( $M = \text{Zn, Co, Ni}$ ). X-ray Powder Diffraction Structure Determination of the Co and Ni Derivatives

M. Dolores Marcos,<sup>†</sup> Pedro Amorós,<sup>\*†</sup> Aurelio Beltrán-Porter,<sup>†</sup>  
 Ramón Martínez-Máñez,<sup>‡</sup> and J. Paul Attfield<sup>§</sup>

UIBCM, Department de Química Inorgànica, Facultat de Química de la Universitat de València, Spain; the Departamento de Química de la Universidad Politécnica de València, Spain; and the Department of Chemistry, University of Cambridge, Lensfield Road, Cambridge CB2 1EW, UK

Received June 29, 1992. Revised Manuscript Received October 30, 1992

Crystalline microporous phosphites of transition metal ions,  $M_{11}(\text{HPO}_3)_8(\text{OH})_6$  ( $M = \text{Zn, Co, Ni}$ ), have been synthesized through soft hydrothermal treatments. The crystal structures of the cobalt and nickel derivatives have been determined by refinement of X-ray powder diffraction data. The cell is hexagonal for both cobalt and nickel compounds (space group  $P6_3mc$ ,  $Z = 1$ ) with  $a = 12.8244$  (4) Å,  $c = 4.9734$  (2) Å, and  $a = 12.6329$  (4) Å,  $c = 4.9040$  (2) Å, respectively. The structure was refined with the Rietveld method, using as a starting model the parameters of the isostructural compound  $\text{Zn}_{11}(\text{HPO}_3)_8(\text{OH})_6$ . The hexagonal structure can be thought of as a pseudomorphic variety of that of dumortierite. It is constructed from zig-zag pyroxene like chains of cationic edge-sharing octahedra which fuse by face-sharing to give double chains. Further connectivity of these double chains through corners results in an open tubular framework in which triangular and hexagonal channels run along the  $c$  axis. The anionic phosphite moieties are located inside the channels. No empty space remains in the smaller triangular ones but the location of phosphite groups on the walls of the bigger hexagonal tunnels occurs in such a way that empty infinite chains of  $\text{H}_6$  face-sharing octahedra result. A strategy of synthesis, which takes into account the hydrolysis of the cationic species, is presented.

Not many years ago, ion exchange behavior was thought to be confined to a very limited number of inorganic compound types. Among these, the best known were clays and zeolites. These compounds are characterized by open structures (lamellar or tubular) that are built up from cations (Al, Si) occupying 4-connected vertices of a three-dimensional net and oxygen atoms occupying 2-connected positions between the 4-connected vertices.<sup>1</sup> However, as work in this area has progressed, other phases (mainly metallic oxides or oxyhydroxides) with 3D frameworks in which the coordination of the cations differs from the typical zeolitic one (4-coordination) have been reported as having also interesting ion exchange behavior. Intercalation and/or exchange chemistry has been also extensively studied in these new materials which deserve attention not only from a theoretical point of view but also because some of them might become commercially useful.<sup>2</sup> In this context, the present work deals with a new family of microporous<sup>3</sup> materials whose framework may be thought of as constituted by octahedrally coordinated transition metal cations and different tetrahedral or

pseudotetrahedral species such as phosphate, phosphite, tellurite and vanadate. The structures of both the already known and the here reported materials in this family can be related to those of the dumortierite<sup>4</sup> and lyonsite<sup>5</sup> minerals, and their main interest lies in the fact that they involve infinite hexagonal channels with window sizes up to ca. 4 Å. The mixed tetrahedral-octahedral structural framework observed in these tubular compounds clearly differs from the well-known aluminosilicate zeolitic ones where the only basic building units are  $\text{AO}_4$  ( $A = \text{Si, Al, or Ge}$ ) tetrahedra.

In fact, the compound which may be considered as the first member of this family,  $\text{Co}_3\text{Te}_2\text{O}_6(\text{OH})_2$ , was prepared 15 years ago,<sup>6</sup> but no other results have been reported until very recent years when several new materials showing related structural motifs have been obtained:  $\text{Zn}_{11}(\text{HPO}_3)_8(\text{OH})_6$ ,<sup>7</sup>  $\text{M}_{12+x}\text{H}_{6-2x}(\text{PO}_4)_8(\text{OH})_6$  ( $M = \text{Co, Ni}$ ),<sup>8</sup> and  $\text{M}_{12-x}\text{H}_{6-2x}(\text{VO}_4)_8(\text{OH})_6$  ( $M = \text{Co, Ni}$ ).<sup>9</sup>

As this family was growing, it seemed us evident that new members might extend it. The stability of this structure and the fact that it may be constructed from different anionic and/or cationic pairs led us to undertake a study whose ultimate aim would be to progress in the

<sup>†</sup> UIBCM, Department de Química Inorgànica, Facultat de Química de la Universitat de València, Dr. Moliner 50, 46100 Burjassot (València), Spain.

<sup>‡</sup> Departamento de Química de la Universidad Politécnica de València, Camino de Vera s/n, 46071 València, Spain.

<sup>§</sup> Department of Chemistry, University of Cambridge, Lensfield Road, Cambridge CB2 1EW, UK.

(1) Smith, J. V. *Chem. Rev.* 1988, 88, 149.

(2) Clearfield, A. *Chem. Rev.* 1988, 88, 125. Clearfield, A. *Inorganic Exchange Materials*; CRC Press: Boca Raton, FL, 1982.

(3) Feng, S.; Tsai, M.; Szu, S. P.; Greenblatt, M. *Chem. Mater.* 1992, 4, 468, and references therein.

(4) Moore, P. B.; Arakai, T. N. *Jb. Miner. Abh.* 1978, 132, 231.

(5) Hughes, J. M.; Starkey, S. J.; Malinconico, M. L.; Malinconico, L. *Am. Mineral.* 1987, 72, 1000.

(6) Perez, G.; Lasserre, F.; Moret, J.; Maurin, M. *J. Solid State Chem.* 1976, 17, 143.

(7) Le Bail, A.; Marcos, M. D.; Amorós, P. *J. Solid State Chem.*, submitted.

(8) Pizarro, J. L. Ph.D. Thesis, U.P.V., Lejona (Bilbao), Spain, 1991.

(9) Le Bail, A.; Lafontaine, M. A.; Perey, G., personal communication.

understanding of the factors governing, besides the window sizes, the electrostatic and crystal field inside the channels. From this point, ionic transport, intercalation, and/or exchange chemistry in these materials might become outstanding.

In the light of the literature data, which show a lack of systematic preparative chemistry (and has usually been carried out in very extreme pressure and temperature conditions), a first step necessary to approach our goal lies in the optimization of the synthetic pathways from a chemically based argument.

In fact, we have been able to rationalize the synthesis of new phosphite derivatives in terms of the hydrolytic processes which the cationic species undergo, and, in this work, we present the synthesis of the isostructural microporous materials  $M_{11}(\text{HPO}_3)_8(\text{OH})_6$  ( $M = \text{Co}, \text{Ni}, \text{Zn}$ ), as well as the structural characterization of the cobalt and nickel derivatives.

### Experimental Section

**Synthesis of  $M_{11}(\text{HPO}_3)_8(\text{OH})_6$ ,  $M = \text{Co}$  (1),  $\text{Ni}$  (2), and  $\text{Zn}$  (3).** 1 was prepared by adding 11.8 mL of KOH 1.4 M to a solution containing 7.92 g of  $\text{CoCl}_2 \cdot 6\text{H}_2\text{O}$  in 10 mL of distilled water. A pink-violet suspension of pH ca. 6 was obtained, and then 40 mL of a 0.6 M solution of  $\text{K}_2\text{HPO}_3$  was dripped over the cobalt suspension while stirring. The suspension became dark, but the pH had no appreciable variation. The mixture was placed in a steel-covered Teflon container filled to 90% of its volume and heated over 3 days with an external temperature of 180 °C. A very fine violet polycrystalline precipitate was separated from the mother liquor by filtration, washed with water (three times, 5 mL) and acetone (three times, 2 mL), and air dried. (Anal.: Co, found 46.9%, calc 46.6%; P, found 18.1%, calc 17.8%).

The nickel derivative (2) was prepared following the same procedure, starting from the equivalent amount of the corresponding nickel salt,  $\text{NiCl}_2 \cdot 6\text{H}_2\text{O}$ . A very fine light green polycrystalline powder was obtained (Anal.: Ni, found 46.3%, calc 46.6%; P, found 17.7%, calc 17.9%).

The synthesis of the zinc compound (3) was described in a previous work.<sup>7</sup> In that case, however, this derivative was obtained as a minority phase together with an unidentified product of very low crystallinity. We can now describe the synthesis of this derivative as bulk material. The procedure is basically the same as for 1 and 2 but involves an important difference: the solution of the chloride salt (5.75 g of  $\text{ZnCl}_2 \cdot 2\text{H}_2\text{O}$  in 10 mL of distilled water) was cooled down in an ice bath, and this temperature was maintained until the addition of the stabilizing anion,  $\text{HPO}_3^{2-}$ . Then, the suspension was treated as in the procedure described above. A white very crystalline powder was obtained. (Anal.: Zn, found 49.0%, calc 49.2%; P, found 17.2%, calc 17.0%).

**Physical Measurements.** Co, Ni, Zn, and P contents in the respective derivatives were determined, after dissolution of the solids in boiling concentrated hydrochloric acid, by atomic absorption spectrophotometry (Perkin-Elmer Zeeman 5000).

X-ray powder diffraction patterns were obtained by means of a Siemens D501 automated diffractometer by using graphite-monochromatized Cu K $\alpha$  radiation, scanned in steps of 0.02° 2 $\theta$  over the angular range 5–110° 2 $\theta$  for 10 s/step and transferred to a VAX computer for analysis.

SEM observations were performed using a HITACHI 2500 microscope.

### Results and Discussion

**Structure Refinement.** The X-ray powder patterns of  $M_{11}(\text{HPO}_3)_8(\text{OH})_6$  ( $M = \text{Co}, \text{Ni}$ ) were indexed from 17 accurately measured reflection positions for compound 1 and 36 for compound 2 by using the TREOR program.<sup>10</sup> A hexagonal primitive cell was obtained in both cases:

**Table I. Final Profile and Structural Parameters for  $\text{Co}_{11}(\text{HPO}_3)_8(\text{OH})_6$  in the Space Group  $P6_3mc$**

Cell Constants					
$a = 12.8244$ (4) Å			$V = 708.37$ (5) Å <sup>3</sup>		
$c = 4.9734$ (2) Å			$Z = 1$		
no. of points in refinements: 5250					
$R_{wp} = 12.7$		$R$ Factors, % $R_p = 9.9$		$R_F = 7.9$	
Structural Parameters					
atom	$x/a$	$y/b$	$z/c$	100 $U_{iso}$ (Å <sup>2</sup> )	site occupancy factor
Co	−0.0772 (2)	0.5689 (2)	0.75	0.38 (8)	0.917
P(1)	−0.16155 (13)	0.16155 (13)	0.2233 (15)	1.1 (2)	1.0
P(2)	$2/3$	$1/3$	0.6744 (2)	0.3 (4)	0.80 (2)
P(3)	$2/3$	$1/3$	0.4987 (2)	0.3 (4)	0.20 (2)
O(1)	0.0762 (9)	0.3430 (8)	0.898 (1)	0.6 (2)	1.0
O(2)	0.2037 (5)	−0.2037 (5)	0.481 (2)	0.6 (2)	1.0
O(3)	0.39847 (16)	−0.39847 (16)	0.0866 (17)	0.6 (2)	1.0
O(4)	0.4675 (6)	−0.4675 (6)	0.551 (3)	0.6 (2)	1.0
H(1)	0.8955	0.1045	0.1300		1.0
H(2)	$2/3$	$1/3$	0.9459		0.80 (2)
H(3)	$2/3$	$1/3$	0.2273		0.20 (2)
H(4)	0.4420	0.5580	0.7203		1.0

compound 1,  $a = 12.820$  (3) Å,  $c = 4.982$  (3) Å, giving the figures of merit  $M_{17} = 15^{11}$  and  $F_{17} = 13$  (0.020, 67);<sup>12</sup> compound 2,  $a = 12.6145$  (16) Å,  $c = 4.8977$  (9) Å, obtaining the figures of merit  $M_{20} = 20^{11}$  and  $F_{20} = 26$  (0.024, 33).<sup>12</sup> No additional systematic absences from the expected ones for the zinc derivative space group ( $P6_3mc$ ) were observed, so this space group was also assumed for the cobalt and nickel compounds.

The structure determination was performed using Rietveld profile refinements with the GSAS program<sup>13</sup> and starting from the coordinates of the  $\text{Zn}_{11}(\text{HPO}_3)_8(\text{OH})_6$  isostructural compound.<sup>7</sup> Using this structural model for all the non-hydrogen atoms the conventional reliability factors dropped rapidly by successive refinement cycles. The refinements were carried out excluding the largely asymmetric (100)(010) peaks in both cases. The refined site occupancy factor for the metallic atoms reached a value very close to the 11/12 ratio corresponding to the expected stoichiometry for these compounds,<sup>7</sup> so both were fixed at the theoretical value of 0.917. At this stage it was found that the  $\text{HPO}_3$  tetrahedra on the 6<sub>3</sub> axis were oriented differently than the same tetrahedra in the Zn compound. From Fourier difference syntheses, these phosphite groups were found to be inverted in the nickel compound, whereas the cobalt derivative was disordered and so the site occupation factors of both orientations were refined.

The positions of the hydrogen atoms were calculated and the distance fixed with standard values for this kind of compounds. The final reliability factors were  $R_{wp} = 12.7$ ,  $R_p = 9.9$ , and  $R_F = 7.9\%$  for compound 1 and  $R_{wp} = 9.5$ ,  $R_p = 7.3$ , and  $R_F = 6.0\%$  for compound 2.

Details of the final refinements and atomic parameters are given in Tables I and II, and selected bond distances and angles are listed in Tables III and IV. Figure 1 shows the observed and calculated patterns for compounds 1 and 2.

**Strategy of Synthesis.** In an attempt to reproduce natural conditions, the synthesis of highly condensed

(11) de Wolf, P. M. *J. Appl. Crystallogr.* 1968, 1, 108.

(12) Smith, G. S.; Snyder, R. L. *Appl. Crystallogr.* 1979, 12, 60.

(13) Larson, A. C.; Von Dreele, R. B. Los Alamos National Laboratory Report No. LA-UR-86-748, 1987.

(10) Werner, P. E. *Krystallographica* 1969, 120, 375.

**Table II. Final Profile and Structural Parameters for  $\text{Ni}_{11}(\text{HPO}_3)_8(\text{OH})_6$  in the Space Group  $P6_3mc$** 

Cell Constants					
$a = 12.6329$ (4) Å			$V = 677.77$ (5) Å <sup>3</sup>		
$c = 4.9040$ (2) Å			$Z = 1$		
no. of points in refinement: 5250					
$R_{wp} = 9.5$		$R$ factors % $R_p = 7.3$		$R_F = 6.0$	
Structural Parameters					
atom	$x/a$	$y/b$	$z/c$	$100U_{iso}$ (Å <sup>2</sup> )	site occupancy factor
Ni	0.92283 (17)	0.56749 (16)	0.75	2.16 (5)	0.917
P(1)	0.8407 (2)	0.1593 (2)	0.2224 (11)	1.61 (5)	1.0
P(2)	$2/3$	$1/3$	0.6797 (14)	1.67 (5)	1.0
O(1)	0.0727 (7)	0.3410 (5)	0.8971 (9)	0.36 (5)	1.0
O(2)	0.2003 (4)	0.7997 (4)	0.4715 (15)	0.36 (5)	1.0
O(3)	0.40051 (19)	0.59949 (19)	0.1034 (16)	0.36 (5)	1.0
O(4)	0.4720 (4)	0.5280 (4)	0.548 (2)	0.36 (5)	1.0
H(1)	0.8955	0.1045	0.1380		1.0
H(2)	$2/3$	$1/3$	0.9512		1.0
H(3)	0.4420	0.5580	0.7203		1.0

**Table III. Selected Interatomic Distances (Å) and Angles (deg) for  $\text{Co}_{11}(\text{HPO}_3)_8(\text{OH})_6$** 

Co Octahedron (Co-O) = 2.144						
Co	O(1)	O(2)	O(4)	O(3)	O(1)	O(4)
O(1)	<b>2.079 (7)</b>	3.251 (8)	4.099 (15)	3.021 (9)	3.008 (10)	3.049 (16)
O(2)	100.1 (5)	<b>2.131 (6)</b>	2.947 (12)	3.189 (9)	3.139 (11)	4.453 (13)
O(4)	162.9 (1)	90.1 (5)	<b>2.038 (12)</b>	2.769 (15)	3.049 (11)	2.877 (19)
O(3)	91.8 (3)	96.5 (3)	83.4 (4)	<b>2.125 (5)</b>	4.275 (8)	2.983 (7)
O(1)	90.1 (4)	93.6 (4)	92.8 (4)	169.2 (3)	<b>2.169 (10)</b>	3.043 (15)
O(4)	87.6 (5)	172.3 (5)	82.3 (3)	84.2 (3)	85.3 (3)	<b>2.319 (12)</b>
P(1) Tetrahedron						
P(1)	H(1)	O(1)	O(1)	O(2)		
H(1)	<b>1.305 (3)</b>	2.342 (11)	2.342 (7)	2.317 (6)		
O(1)	109.5 (4)	<b>1.517 (7)</b>	2.444 (8)	2.490 (9)		
O(1)	109.5 (4)	107.5 (3)	<b>1.517 (7)</b>	2.490 (110)		
O(2)	108.4 (3)	111.0 (4)	111.0 (4)	<b>1.425 (5)</b>		
P(2) Tetrahedron						
P(2)	H(2)	O(3)	O(3)	O(3)		
H(2)	<b>1.350 (1)</b>	2.299 (7)	2.300 (7)	2.296 (7)		
O(3)	106.8 (2)	<b>1.522 (4)</b>	2.507 (4)	2.504 (3)		
O(3)	106.8 (2)	112.0 (1)	<b>1.511 (4)</b>	2.501 (4)		
O(3)	106.9 (2)	112.1 (2)	111.9 (2)	<b>1.511 (4)</b>		
P(3) Tetrahedron <sup>a</sup>						
P(3)	H(3)	O(3)	O(3)	O(3)		
H(3)	<b>1.350 (1)</b>	2.300 (7)	2.300 (7)	2.296 (7)		
O(3)	106.8 (4)	<b>1.511 (5)</b>	2.507 (4)	2.504 (3)		
O(3)	106.8 (4)	112.0 (2)	<b>1.5111 (5)</b>	2.501 (4)		
O(3)	106.8 (4)	112.1 (3)	111.8 (3)	<b>1.511 (5)</b>		
Octahedra Sharing						
face		edge		corner		
Co-Co	2.757 (4)	Co-Co	2 × 3.020 (3)	Co-Co	3.548 (4)	
				Co-Co	2 × 4.089 (3)	

<sup>a</sup> P(2)-P(3) = 0.874 (2) Å.

materials has been usually accomplished in the laboratory by means of vigorous hydrothermal treatments.<sup>14</sup> Whereas these procedures give many times "very profitable yields", mainly from a crystallographic point of view (several crops of single crystals after only "one" reaction),<sup>15</sup> they lack, in

**Table IV. Selected Interatomic Distances (Å) and Angles (deg) for  $\text{Ni}_{11}(\text{HPO}_3)_8(\text{OH})_6$** 

Ni Octahedron						
Ni	O(1)	O(2)	O(4)	O(3)	O(1)	O(4)
O(1)	<b>2.067 (4)</b>	3.009 (9)	2.936 (7)	4.123 (6)	2.923 (8)	3.010 (10)
O(2)	91.2 (2)	<b>2.095 (3)</b>	2.998 (9)	3.101 (8)	3.144 (7)	4.306 (9)
O(4)	91.1 (2)	94.3 (3)	<b>1.995 (8)</b>	2.682 (11)	4.037 (10)	2.741 (13)
O(3)	170.0 (2)	97.7 (2)	83.8 (2)	<b>2.022 (5)</b>	3.004 (6)	2.803 (5)
O(1)	88.6 (2)	98.2 (3)	1647.6 (3)	94.6 (2)	<b>2.117 (6)</b>	2.936 (11)
O(4)	88.0 (2)	175.2 (2)	81.0 (2)	82.7 (2)	86.5 (3)	<b>2.215 (8)</b>
P(1) Tetrahedra						
P(1)	H(1)	O(1)	O(1)	O(2)		
H(1)	<b>1.269 (5)</b>	2.286 (6)	2.286 (6)	2.250 (7)		
O(1)	109.6 (4)	<b>1.523 (4)</b>	2.471 (8)	2.512 (7)		
O(1)	109.6 (3)	108.4 (3)	<b>1.523 (4)</b>	2.512 (7)		
O(2)	107.1 (4)	111.1 (3)	111.1 (4)	<b>1.525 (3)</b>		
P(2) Tetrahedra						
P(2)	H(2)	O(3)	O(3)	O(3)		
H(2)	<b>1.331 (1)</b>	2.251 (7)	2.251 (7)	2.251 (7)		
O(3)	104.3 (2)	<b>1.517 (2)</b>	2.546 (4)	2.546 (3)		
O(3)	104.3 (2)	114.1 (1)	<b>1.517 (2)</b>	2.546 (4)		
O(3)	104.3 (2)	114.2 (1)	114.1 (1)	<b>1.517 (2)</b>		
Octahedra Sharing						
face		edge		corner		
Ni-Ni	2.681 (4)	Ni-Ni	2 × 2.977 (3)	Ni-Ni	3.548 (4)	
					2 × 4.089 (3)	

most cases, any clear systematic approach and, not infrequently, lead to irreproducible results.<sup>16</sup> Thus, a relevant aspect of the procedure here reported lies in the systematic, and reproducible, synthesis of condensed phosphites by using "soft chemistry" techniques.

In fact, the chemistry of phosphite-containing materials has not been extensively studied. The number of published works on the subject is relatively small, and they mainly deal with specific preparative and/or structural aspects.<sup>17</sup> In particular, no systematic study of the influence of the conditions of synthesis has been reported. When thinking about the synthesis of transition metal derivatives of this low oxidation state oxophosphoric acid, it becomes necessary to consider, besides the redox chemistry of the anionic species, problems originating from the hydrolytic processes which the cationic counterpart may undergo, problems that, obviously, do not arise in the synthesis of the better known alkaline or alkaline-earth metal salts.<sup>18</sup>

Our synthetic approach, which has allowed us to obtain not only the title compounds but also other related derivatives such as  $\text{M}(\text{HPO}_3)(\text{H}_2\text{O})$  ( $\text{M} = \text{Co},^{19} \text{Ni},^{20} \text{Zn}^{20}$ ), is based on a very simple idea focused on these hydrolytic processes: that the resulting cationic network in the final solid would be essentially controlled by the cationic aggregates present in the mother solution.

Actually, the aqueous solution hydrolytic chemistry of the transition metals is, in general, very complex. A number of species, with variable condensation degrees, are known for different metals, but two variables, pH and

(16) Lii, K. H.; Tsai, H. J. *Inorg. Chem.* 1991, 30, 446.(17) Loub, J.; Kratochvil, B. *Chem. Listy* 1987, 81, 337.(18) See, for example: Durand, J.; Loukili, M.; Tijani, N.; Rafiq, M.; Cot, L. *Eur. J. Solid State Inorg. Chem.* 1988, 25, 297.(19) Marcos, M. D.; Gomez-Romero, P.; Amorós, P.; Sapiña, F.; Beltrán-Porter, D.; Navarro, R.; Rillo, C.; Lera, F. *J. Appl. Phys.* 1990, 67, 5998.(20) Marcos, M. D.; Gomez-Romero, P.; Marcos, M. D.; Amorós, P.; Ibañez, R.; Beltrán-Porter, D.; Navarro, R.; Rillo, C.; Lera, F. *Eur. J. Solid State Inorg. Chem.* 1989, 26, 603.

(20) Marcos, M. D., unpublished results.

(14) Rabenau, A. *Angew. Chem., Int. Ed. Engl.* 1985, 24, 1026.(15) Demazeau, G.; Fabritchnyi, P. B.; Legasov, V. A.; Etourneau, J.; Hagenmuller, P. *Russ. J. Inorg. Chem.* 1989, 34, 1. Lee, C. S.; Lii, K. H. *J. Solid State Chem.* 1991, 92, 362.(15) Lii, K. H.; Tsai, H. J. *J. Solid State Chem.* 1991, 91, 331.

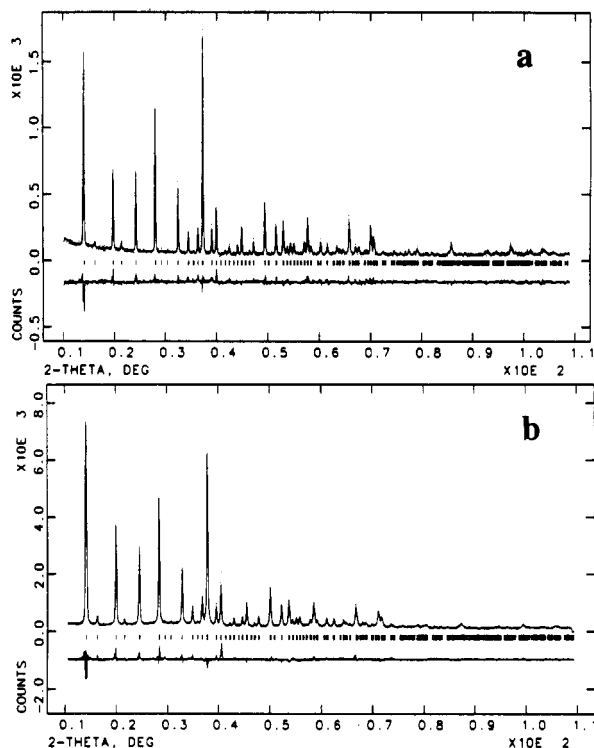


Figure 1. Observed, calculated and difference X-ray diffraction patterns; (a)  $\text{Co}_{11}(\text{HPO}_3)_8(\text{OH})_6$  (1); (b)  $\text{Ni}_{11}(\text{HPO}_3)_8(\text{OH})_6$  (2).

metal ion concentration ( $C_M$ ), mainly determine the ranges of stability of the various condensed species.<sup>21</sup> So, by adjusting the conditions of syntheses at different points of the diagrams, it might be possible to obtain materials with different cationic condensation degrees.

Following this idea, the preparation of solids where oxo groups do not play a bridging role between cations should be possible starting from solutions having low pH and  $C_M$  values, given that the prevailing cationic species in aqueous solution under these conditions are of the type  $\text{M}(\text{H}_2\text{O})_m^{n+}$ . This is in fact the case in the synthesis of  $\text{Co}(\text{HPO}_3)(\text{H}_2\text{O})$  previously described<sup>19</sup> and then extended to  $\text{M}(\text{HPO}_3)(\text{H}_2\text{O})$  ( $\text{M} = \text{Ni}, \text{Zn}$ ).<sup>20</sup> On the contrary, by carrying out the synthesis at intermediate values of pH and high concentrations of the metallic ions (see Experimental Section), we obtain the title compounds,  $\text{M}_{11}(\text{HPO}_3)_8(\text{OH})_6$  ( $\text{M} = \text{Co}, \text{Ni}$ , and  $\text{Zn}$ ), characterized by the presence of cationic chains (see below) in which  $\text{OH}^-$  groups connect four metallic atoms. This kind of chains could be constructed from the initially formed dimeric,  $\text{M}_2(\text{OH})^{3+}$ , or tetrameric,  $\text{M}_4(\text{OH})_4^{4+}$ , cationic entities which have been recognized as principal products of the hydrolysis for similar pH and  $C_M$  conditions.<sup>21</sup>

The syntheses of the zinc compounds, however, present an additional problem due to its high tendency to form tetrahedral species, both in solution<sup>22</sup> and in solid state.<sup>23</sup> It is because of this fact that the syntheses have been performed maintaining the temperature of the starting solutions close to 0 °C. Low-temperature values favor the formation of octahedral species,<sup>22</sup> and these become

stabilized after addition of phosphite anions. The subsequent hydrothermal treatment does not modify this situation, i.e., the octahedral species do not evolve toward tetrahedral ones, as was observed when working in conditions similar to those used for the cobalt and nickel derivatives.

Nonetheless, it must be stated that, in all cases, the only aim fulfilled by applying the hydrothermal treatment here described is the improvement of the crystallinity of the materials. In fact, the synthesis of the title compounds,  $\text{M}_{11}(\text{HPO}_3)_8(\text{OH})_6$  ( $\text{M} = \text{Co}, \text{Ni}$  and  $\text{Zn}$ ), can equally be achieved by heating the precursor suspensions under reflux during several days, although powdered products of very low crystallinity result in this case.

In short, all this occurs as if the addition of the anionic species to the fresh aquahydroxydic slurry induces further condensation of the preformed cationic entities, benefitting from the coordinating ability of the incoming phosphite groups. The resulting granular amorphous precipitates then evolve smoothly (by refluxing or through soft hydrothermal treatment) to give the final crystalline powders.

From these ideas, it becomes possible to understand the experimental results obtained when the synthesis of the zinc derivative was performed as described in ref 7 (i.e., when the addition of phosphite was made at adequate pH and  $C_M$  values but at room temperature) in contrast to that here reported. As shown in Figure 2a, that synthesis led to big and well-formed hexagonal single crystals of  $\text{Zn}_{11}(\text{HPO}_3)_8(\text{OH})_6$ , although the yield of this phase was very low and the few crystals obtained were immersed in an unidentified amorphous majority phase. This is a consequence of the very few octahedral cationic nucleation centers present in the zinc suspension at room temperature. By contrast, the synthesis reported here leads to monophasic materials showing (see Figure 2b,c) oval polycrystalline grains that are very homogeneously sized (4–9  $\mu\text{m}$ ). As can be noted, the clusters in the granular aggregates of the zinc derivatives are formed by crystals which only differ from the big ones in Figure 2a in their size, a fact that may be related to the kinetics of crystallization owing to the presence of a raised number of nucleation centers.

**Description of the Structure.** Shown in Figure 3 is a projection of the structure of  $\text{M}_{11}(\text{HPO}_3)_8(\text{OH})_6$  ( $\text{M} = \text{Co}, \text{Ni}$ ) along the (001) direction. The structure closely resembles that found for the homologous zinc derivative.<sup>7</sup> Regarding its general features, the intricate 3D framework in these compounds may formally be described in two complementary ways:

(a) The structural arrangement can be seen as dictated by the packing of cationic  $\text{MO}_6$  octahedra, where four oxygen atoms ( $2 \times \text{O}(1), \text{O}(2)$  and  $\text{O}(3)$ ) belong to phosphite pseudotetrahedra and the two remaining ones ( $2 \times \text{O}(4)$ ) to hydroxyl groups. Each  $\text{MO}_6$  octahedron shares two edges ( $\text{O}(1)–\text{O}(4)$ ) with other two at  $z \pm 1/2$  in such a way that an infinite zig-zag pyroxene-like ( $\text{MO}_4$ )<sub>n</sub> chain results. Formal condensation two by two of these equivalent chains, which fuse by sharing a face ( $\text{O}(3)–\text{O}(4)–\text{O}(4)$ ) of each octahedron with another octahedron at the same  $z$  level, gives infinite ( $\text{M}_4\text{O}_{12}$ )<sub>n</sub> double chains running along the  $c$  axis. Alternatively, these double chains may be thought of as built up of dimeric ( $\text{M}_2\text{O}_9$ ) entities (two  $\text{MO}_6$  octahedra sharing the  $\text{O}(3)–\text{O}(4)–\text{O}(4)$  face) linked through two common edges ( $\text{O}(1)–\text{O}(4)$ ) to give the infinite chains of dimers of composition ( $\text{M}_4\text{O}_{12}$ )<sub>n</sub>.

(21) Baes, C. F., Jr.; Mesmer, R. E. *The Hydrolysis of Cations*; Wiley: New York, 1976.

(22) Sillén, L. G.; Martell, A. E. *Stability Constants of Metal-Ion Complexes*; The Chemical Society: Oxford.

(23) Sandomirskii, P. A.; Klientova, G. P.; Simonov, M. A.; Belov, N. V. *Dokl. Akad. Nauk SSSR* 1977, 236, 597. Iijima, K.; Marumo, F.; Takei, H. *Acta Crystallogr.* 1948, B38, 1112. Whitaker, A. *Acta Crystallogr.* 1975, B31, 2026.

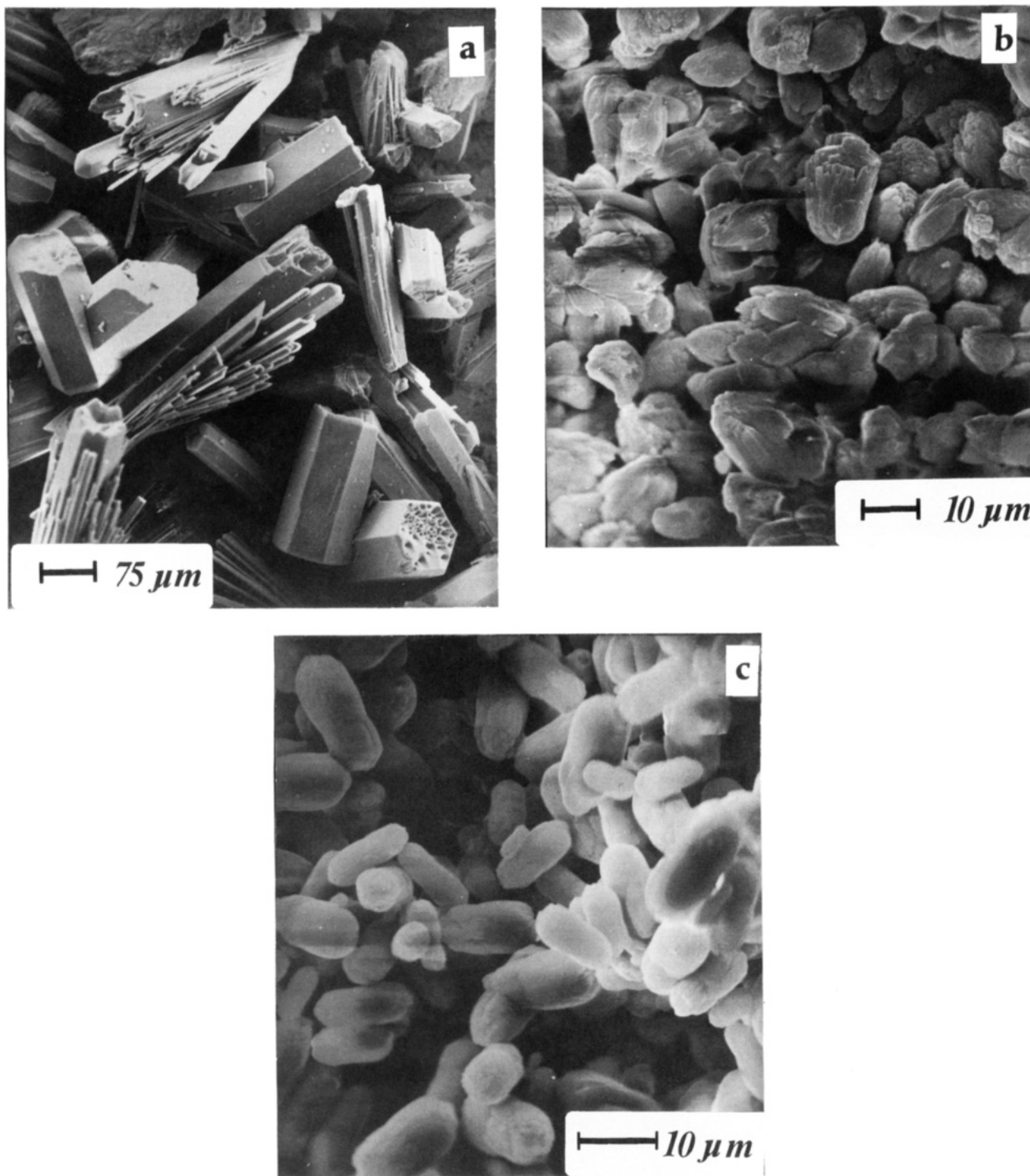


**Figure 2.** SEM images of (a)  $\text{Zn}_{11}(\text{HPO}_3)_8(\text{OH})_6$  single crystals, (b)  $\text{Zn}_{11}(\text{HPO}_3)_8(\text{OH})_6$  powder, and (c)  $\text{Co}_{11}(\text{HPO}_3)_8(\text{OH})_6$  powder.

The final open tridimensional array of octahedra would result from the connection of each one of these double chains to other four equivalent adjacent ones by corner sharing.

In their resulting hexagonal arrangement, the octahedra delimit two kinds of channels. The smaller triangular ones, surrounded by three  $(\text{M}_4\text{O}_{12})_n$  chains, are occupied by 2/8 of the  $\text{HPO}_3^{2-}$  (P(2)) pseudotetrahedral groups. The remaining (6/8) phosphite groups (P(1)) are located on the walls of the larger hexagonal channels.

(b) The structure of the title compounds,  $\text{M}_{11}(\text{HPO}_3)_8(\text{OH})_6$ , is closely related to that of the dumortierite mineral, a complex oxyborosilicate of aluminum,  $\text{Al}_7\text{O}_3(\text{BO}_3)_8$ -

$(\text{SiO}_4)_3$ , whose structure was analyzed in detail by Moore and Araki.<sup>4</sup> As in the dumortierite case, the structure of the title compounds "can be considered as an elegant version of the design on the semi-regular planar net {6.4.3.4}."<sup>4</sup> This net is shown in Figure 4, and an idealization of the structure of  $\text{M}_{11}(\text{HPO}_3)_8(\text{OH})_6$  results from the placement of the A, B, and C designs over the net. In fact, these designs correspond to structural modules found in  $\text{M}_{11}(\text{HPO}_3)_8(\text{OH})_6$  (see Figure 5). Thus, as shown in Figure 6, the A region corresponds to the  $(\text{M}_4\text{O}_{12})_n$  double chains, B to  $\text{HPO}_3^{2-}$  (P2) pseudotetrahedral groups (2/8 of the whole phosphite groups in the formulae) and C to  $[\text{H}_6]_n$  empty chains plus its surrounding "pinwheel" of



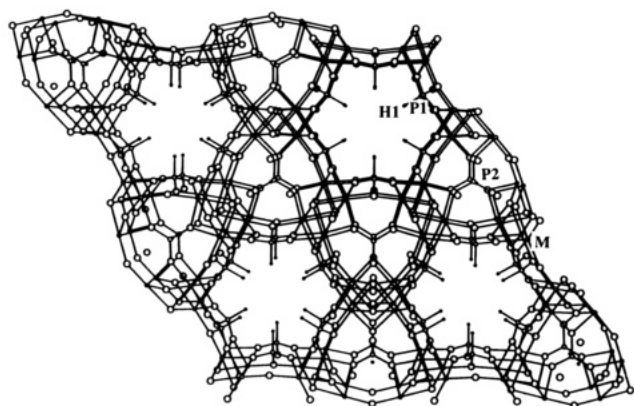


**Figure 3.** Projection down *c* of the structure of  $M_{11}(\text{HPO}_3)_8(\text{OH})_6$  ( $M = \text{Co}, \text{Ni}$ ). Particularities of each compound have been eliminated for clarity.

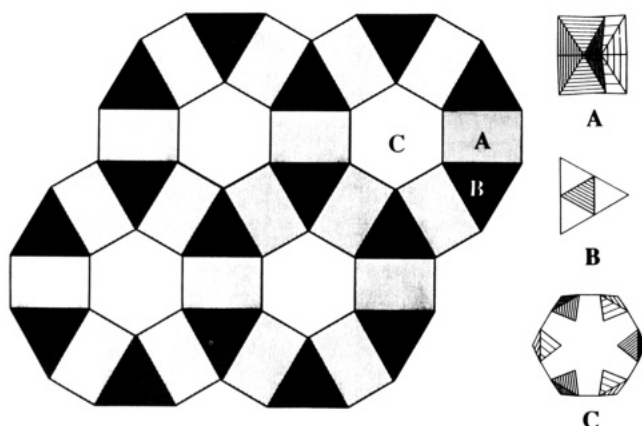


**Figure 4.** Regular planar {6.4.3.4} net and the three designs (A, B, and C) representing modules found in  $M_{11}(\text{HPO}_3)_8(\text{OH})_6$  ( $M = \text{Zn}, \text{Co}$ , and  $\text{Ni}$ ). Appropriate placement of these designs over the net leads to an idealized structure of the title compounds.

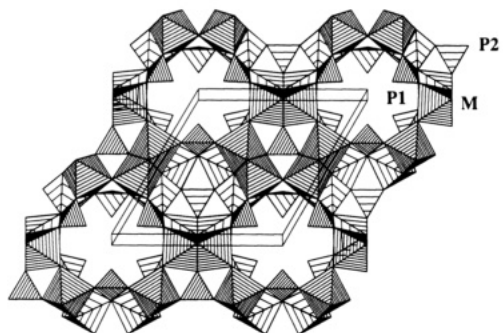


**Figure 5.** Polyhedral (STRUPLO) representation of  $M_{11}(\text{HPO}_3)_8(\text{OH})_6$  ( $M = \text{Co}, \text{Ni}$ ) along (001) as resulting from the replacement of the A, B, and C modules in the {6.4.3.4} net. The distinctly dashed  $[\text{MO}_6]$  octahedra and  $[\text{HPO}_3]$  pseudotetrahedra are at different *z* levels (zinc atoms at  $z = 0$  and  $z = 1/2$ ).

the remaining portions of six  $\text{HPO}_3^{2-}$  ( $\text{P}(1)$ ) pseudotetrahedra (i.e., the  $[\text{H}_6]_n$  unit is defined by six hydrogen atoms, octahedrally arranged, which belong to six different  $\text{HPO}_3^{2-}$  groups, 6/8 of the whole).

Paying attention to the  $[\text{MO}_6]$  octahedra, these show a notable distortion in both cases, as expected from the sharing of structural elements. Thus, the M–O bond lengths vary in the ranges 2.038–2.319 and 1.995–2.215 Å for the Co and Ni derivatives, respectively. In both cases, these maximum and minimum distances correspond to the M–O(4) bonds, as this oxygen atom is shared by four cations in the double chain. A rough estimation of the distortion may be made by using the equation  $\Delta = 1/6 \sum$

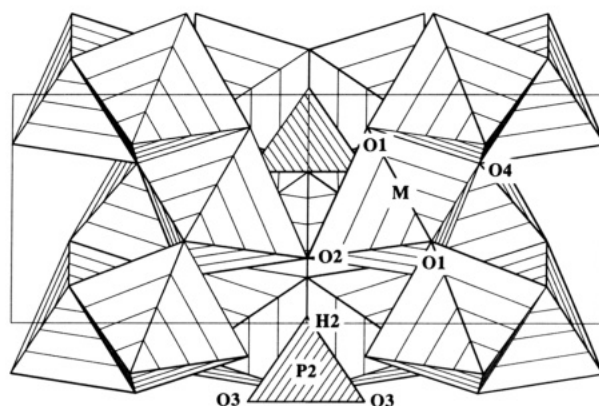


**Figure 6.** Partial view of the structure of  $M_{11}(\text{HPO}_3)_8(\text{OH})_6$  ( $M = \text{Co}, \text{Ni}$ ) perpendicular to the *c* axis showing the arrangement of A and B modules.

**Table V.** Valence Bond Analysis for  $M_{11}(\text{HPO}_3)_8(\text{OH})_6$  ( $M = \text{Co}, \text{Ni}$ ) Using the Zachariassen Law

	Co	P(1)	P(2) or P(3)	$\Sigma$
O(1)	0.35 0.28	1.33		1.96
O(2)	0.31 × 2	1.31		1.93
O(3)	0.31 × 2		1.35 × 3	1.97
O(4)	0.40 × 2 0.18 × 2			1.16
$\Sigma$	1.84	3.97 <sup>a</sup>	4.05 <sup>a</sup>	
	Ni	P(1)	P(2)	$\Sigma$
O(1)	0.33 0.29	1.31 × 2		1.93
O(2)	0.3 × 2	1.31		1.92
O(3)	0.34 × 2		1.33 × 3	2.01
O(4)	0.40 × 2 0.22 × 2			1.24
$\Sigma$	1.88	3.93 <sup>a</sup>	3.99 <sup>a</sup>	

<sup>a</sup> The calculation does not include the 1 valence unit corresponding to the P–H bond.

$[(R_i - R)/R]^2$ , where  $R_i$  = individual bond length and  $R$  = average bond length.<sup>24</sup> The calculated values,  $\Delta(\text{Co}) = 0.171$  and  $\Delta(\text{Ni}) = 0.087$ , show that the distortion for the cobalt compound is significantly larger (in accordance with its Jahn–Teller activity) than that in  $\text{Zn}_{11}(\text{HPO}_3)_8(\text{OH})_{11}$  ( $\Delta(\text{Zn}) = 0.105$ ), which, in turn, is similar to that found for the nickel compound. In both cases, however, the observed distortion for the  $\text{MO}_6$  octahedra ( $M = \text{Co}, \text{Ni}$ ) is greater than the calculated one for other related materials such as  $M(\text{HPO}_3)(\text{H}_2\text{O})$ , ( $M = \text{Co}$  ( $\Delta = 0.054$ ),  $\text{Ni}$ , ( $\Delta = 0.031$ )),<sup>19,20</sup> a fact that is due to the higher steric constraints related to condensation of octahedra.

On the other hand, the bond valence analysis of the M–O bonds, carried out using the Zachariassen law<sup>25</sup> (see Table V), shows a slightly deficient valence for the metallic atoms (1.84 and 1.88 v.u. for the cobalt and nickel material, respectively). The intermetallic distances (see Tables III and IV) clearly show that there is no metal–metal bond, and this departure might be explained by taking into account the long M–O(4) distance mentioned above. In fact, although it was not possible to locate the hydrogen atoms from the X-ray analysis, the bond valence calculations show a very deficient valence for the O(4) atoms.

(24) Shannon, R. D. *Acta Crystallogr.* **1976**, A32, 751.

(25) Zachariassen, W. H. J. *Less Common Met.* **1978**, 62, 1. Brown, I. D. In *Structure and Bonding in Crystals*; O'Keeffe, M., Navrotsky, A., Eds.; Academic Press: New York, 1981; Vol. 2, p 1.

(26) Shannon, R. D.; Prewitt, C. T. *Acta Crystallogr.* **1969**, B25, 925.

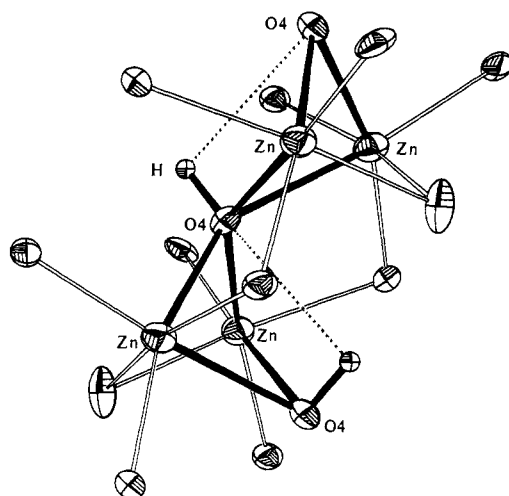


**Figure 7.** ORTEP view of the A modules in the zinc derivative  $(\text{Zn}_{11}(\text{HPO}_3)_8(\text{OH})_6)$  including the hydrogen bonding network involving the O(4)-H groups.

It is this result which clearly suggests the existence of OH groups, as occur in the Zn compound.<sup>7</sup> Hence, the hydrogen-bonding network in the title compounds must be similar to that found in the Zn derivative (see Figure 7).

The variation of the unit cell dimensions over the  $\text{M}_{11}(\text{HPO}_3)_8(\text{OH})_6$  ( $\text{M} = \text{Zn}, \text{Ni}, \text{Co}$ ) series correlates nicely with the cation size. Changes found in the  $a$  and  $c$  axes and that of the volume of the cell have been plotted in Figure 8. As can be noted, the cell volume varies linearly with the ionic radius of the cation. Dealing with the cell parameters, the variation is less pronounced for the  $c$  axis than for  $a$ . In fact the pillaring of the octahedra along the  $c$  axis is so compact that few variations are possible. The result is a very small slope whose order of magnitude is the same as that of the cationic radii variation. Larger changes are detected in the  $ab$  plane, which is attributable to the smaller rigidity of the structure along these directions.

On the other hand, it is difficult to disentangle the influence of the different factors leading to the main structural difference among these three materials, i.e., the change in the  $\text{HPO}_3^{2-}$  (P(2), P(3)) groups position. Thus, if we draw an imaginary plane across the three equivalent O(3) atoms of these P(2)-phosphites, we find that in the nickel derivative both Ni and P(2) atoms stay at the same side of this plane (cis position). On the contrary, in the case of the zinc compound the respective Zn and P(2) atoms are located at opposite sides of the plane (trans position). So, we can say that these phosphite pseudotetrahedra have become inverted, like an umbrella, from one material to the other. In the cobalt derivative the situation is intermediate, and we have found some disorder in the location of P(2) phosphorus atoms: there are 20% of the tetrahedra in the trans position (as in the Zn compound) and 80% in the cis position (as in the Ni one). It should be possible to relate these different situations to the ionic radii variation, given that, as mentioned above, this variation results in concomitant changes of the  $a$  cell parameter and in the dimensions of the channels which accommodate the phosphite groups. Looking at the O(3) atoms, which are coordinated to two metal atoms and one phosphorus (P(2)) atom, it might initially be expected, except for the steric constraints resulting from the cation condensation, that all three bonds involving each O(3)

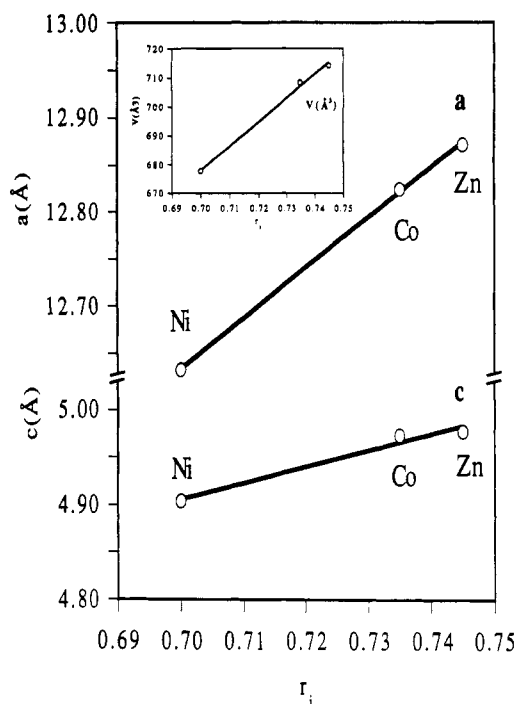


**Figure 8.** Dimensional changes in the  $a$  and  $c$  axes in relation to the variation of the ionic radii<sup>26</sup> in the compounds  $\text{M}_{11}(\text{HPO}_3)_8(\text{OH})_6$  ( $\text{M} = \text{Zn}, \text{Co}, \text{and Ni}$ ). In the inset, variation of the cell volume.

atom should be coplanar (it must be noted that the O(3)-P(2) bond distances, ranging from 1.511 to 1.517 Å, are very close to those found for  $\text{Na}_2\text{HPO}_3$ , 1.522 and 1.525 Å,<sup>27</sup> i.e., the O(3)-P(2) bonds have a certain double-bond character). In practice, the situation in the zinc derivative does not differ to a great extent from this hypothesis, and the departure of the O(3) atom from the plane defined by P(2) and both Zn atoms is +0.193 (5) Å. This is not the case in the nickel compound in which the O(3) atoms are 0.551 (1) Å below the Ni-P(2)-Ni planes, i.e., the O(3) environment becomes pyramidal. This different arrangement, which results from the pseudotetrahedra inversion we are dealing with, might be understood in terms of the compression of the cell, which, in turn, implies a contraction of the triangular channels.<sup>28</sup> This contraction would result in a mismatched orientation of the phosphite ligand group orbitals and the metallic ones (for the trans configuration) and, as the cation octahedra are subject to steric constraints due to their condensation, the more flexible phosphite groups may invert to keep the best possible overlap.

### Concluding Remarks

From a structural point of view, the tubular phosphites reported here constitute a nice example of the validity of the previous Moore and Araki crystallographic analysis:

(27) Brodalla, D.; Goeters, C.; Kniep, R.; Mootz, D.; Wunderlich, H. *Z. Anorg. Allg. Chem.* 1978, 439, 265.

(28) A quantitative parametrization of the dimensions of these channels is not evident, as the variation along the (001) direction of the geometry of the channels referred to as triangular is complex. A transversal section would show a chair, hexane-like,  $[3 \times \text{O}(3)-\text{O}(2)]$  profile whose propagation along  $c$  varies with both the intradimeric and interdimeric dihedral angles. Thus, there are many parameters involved in the real shape and the size of the channels. However, an estimate of the mentioned contraction might be furnished, for example, by the distance between O(4) atoms located at the same  $z$  level, which decreases from 5.459 Å in the Zn derivative to 5.255 Å in the nickel compound.

when hexagonal dimorphs of dumortierite have been found they crystallise in space group  $P6_3mc$ .<sup>4,6</sup>

In the light of the secondary role played by the anionic moieties in this rigid structure,<sup>4</sup> which, in turn, would imply a wide chemical versatility controlled by the cation hydrolysis, it is not unreasonable to expect that new members of this structurally relevant family may be rapidly prepared, although further work is needed to put the Moore and Araki analysis on a chemical (electronic) basis. Preliminary studies on the exchange chemistry of these

types of materials are currently in progress.

**Acknowledgment.** This work was supported by the DGICYT under Grant PB91-0459 and the Institució Valenciana d'Estudis i Investigació (IVEI). M.D.M. thanks the Spanish Ministerio de Educación y Ciencia for a FPI fellowship to visit the Chemical Crystallography Laboratory, Oxford, where the structure refinements were performed. The SCME of the University of Valencia (Spain) is acknowledged for SEM facilities.